


Structural and magnetic properties of FeCoC system obtained by mechanical alloying

A. I. Rincón Soler¹ · R. R. Rodríguez Jacobo²  ·
M. H. Medina Barreto¹ · B. Cruz-Muñoz¹

© Springer International Publishing Switzerland 2017

Abstract Fe_{96-x}Co_xC₄ ($x = 0, 10, 20, 30, 40$ at. %) alloys were obtained by mechanical alloying of Fe, C and Co powders using high-energy milling. The structural and magnetic properties of the alloy system were analyzed by X-ray diffraction, Scanning Electron Microscopy (SEM), Vibrating Sample Magnetometer (VSM) and Mössbauer Spectrometry at room temperature. The X-ray diffraction patterns showed a BCC-FeCoC structure phase for all samples, as well as a lattice parameter that slightly decreases with Co content. The saturation magnetization and coercive field were analyzed as a function of Co content. The Mössbauer spectra were fitted with a hyperfine magnetic field distribution showing the ferromagnetic behavior and the disordered character of the samples. The mean hyperfine magnetic field remained nearly constant (358 T) with Co content.

Keywords FeCoC · Soft magnetic · Mechanical alloying

1 Introduction

Iron-Cobalt alloys are known to have many applications in a wide variety of areas due to their excellent magnetic properties (High magnetization saturation, low coercivity, high

This article is part of the Topical Collection on *Proceedings of the 15th Latin American Conference on the Applications of the Mössbauer Effect (LACAME 2016), 13–18 November 2016, Panama City, Panama*
Edited by Juan A. Jaén

✉ R.R. Rodríguez Jacobo
rrrodriguez@uao.edu.co

¹ Fac. de Ciencias, Depto. de Física, Universidad Tecnológica de Pereira, Pereira 660003, Colombia

² Fac. de Ciencias Básicas, Depto. de Física, Universidad Autónoma de Occidente, A.A. 2790, Cali, Colombia

Curie temperatures, high permeability, low hysteresis loss and low eddy currents loss but high electric permeability) [1, 2]. On the other hand, the process of mechanical alloying is one of the best techniques to synthesize powders and obtain solid solutions in a desired stoichiometry and it is widely used in the preparation of various metal-metal systems, including iron-cobalt systems [3]. This process is accompanied by a strong deformation of crystalline lattices for the processed powders. Moumeni et al. [4] reported that a small number of hours of milling are enough to obtain a solid solution in which the Co dissolves completely in the iron matrix. Nanostructured FeCo alloys have been subject of considerable interest due to their exceptional magnetic properties [5, 6]. The addition of a third element to FeCo alloys influences significantly their several physical properties, for example, carbon, molybdenum, tungsten, tantalum, niobium and nickel are effective in improving the ductility of FeCo alloys [7, 8].

In this work, the structural and magnetic properties of $\text{Fe}_{96-x}\text{Co}_x\text{C}_4$ ($x=0, 10, 20, 30, 40$ at.%) alloy system are analyzed as a function of cobalt content. It will be used in future works, as targets for the preparation of low dimensional systems

2 Experimental

Milled samples were obtained from pure element powders (iron 99.9%, cobalt 99.9% and carbon 99.95%), using a Pulverisette 5 high energy planetary ball mill during 20 hours. The milling speed was 280 rpm and the process was carried out using a sequence of 60 minutes milling and 30 minutes resting with a ball to powder ratio of 14:1. The elemental powders were weighted in the desired stoichiometric relation and mixed in a small flask, then transferred into the vials, under an argon atmosphere.

XRD measurements were performed in a Rigaku D'Max 2100 diffractometer with $\text{CuK}\alpha$ radiation ($\lambda = 1.5406 \text{ \AA}$) and the patterns were refined using General Structure Analysis System (GSAS) software [9] which is based on the Rietveld method. ^{57}Fe Mössbauer experiments were performed at room temperature in transmission geometry using a conventional spectrometer with a constant acceleration mode and ^{57}Co source diffused into a rhodium matrix. The analysis of the Mössbauer spectra was done using the Mosfit program (J. Teillet, F. Varret, unpublished Mosfit Program University of Maine) and the values of isomer shift were referred to α -Fe at 300 K. Besides, the magnetic behavior of the system was quantified using a VersaLab vibrating-sample magnetometer (VSM) at room temperature and with a magnetizing field of 30 kOe and sample step of 0.2 Oe. The morphology and chemical structure of the system were recognized using Scanning Electron Microscopy (SEM) and Energy Dispersive Spectroscopy (EDX), both techniques on a Philips ESEM XL-30.

3 Results and discussion

3.1 Energy dispersive X-ray analysis

For milled powders of the $\text{Fe}_{96-x}\text{Co}_x\text{C}_4$ ($x=0, 10, 20, 30$ and 40 at. % Co), an Energy Dispersive X-ray Analysis was used to quantify the atomic and weight percentage of the elements present in each sample. The values in Table 1 show an agreement in the stoichiometry of the system before and after milling process. Some impurities, like oxygen and aluminum, were detected and attributed to reactions presented during the mechanical process of milling.

Table 1 Theoretical and experimental weight percentage for FeCoC system

Fe _{96-X} Co _X C ₄ (at. %)	Theoretical (wt. %)		EDX (wt. %)			
	Fe	Co	Fe (±5)	Co (±7)	O (±1)	Al (±0.5)
0	99.11	0	94	0	3	0.5
10	88.28	10.83	84	10	3	
20	77.58	21.54	73	20	4	
30	66.99	32.13	64	30	3	
40	56.53	42.61	57	36	4	

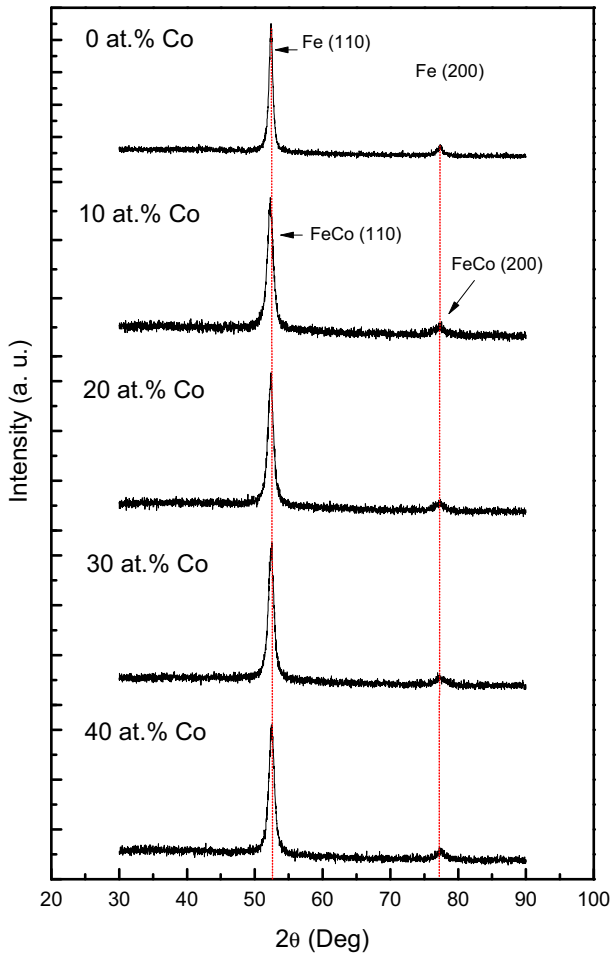


Fig. 1 XRD patterns of the Fe_{96-x}Co_xC₄ alloys as a function of Co content

3.2 X-ray diffraction

XRD patterns of Fe_{96-x}Co_xC₄ as a function of Co concentration are shown in Fig. 1. These patterns reveal a BCC structure and the complete disappearing of FCC and HCP-Co peaks

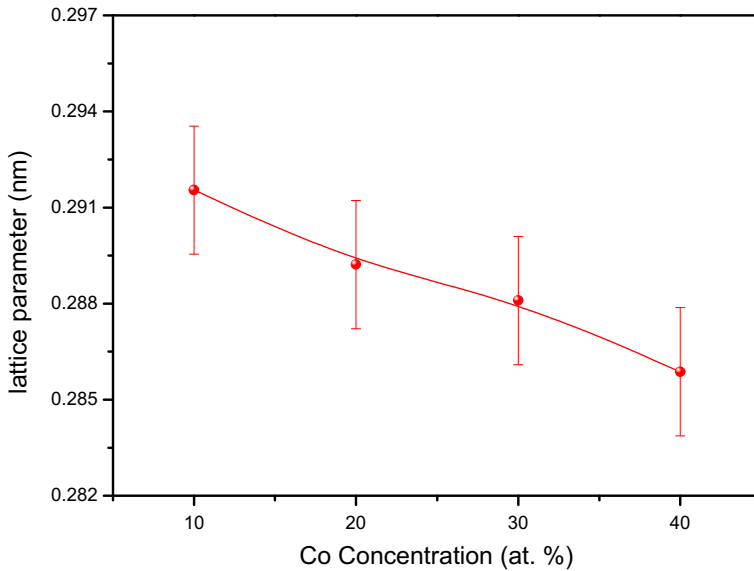


Fig. 2 Lattice parameter as a function of Co Content

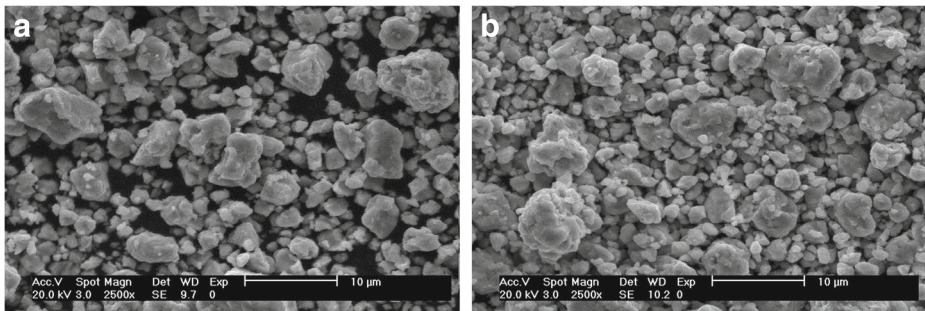


Fig. 3 SEM micrograph of (a) $\text{Fe}_{86}\text{Co}_{10}\text{C}_4$ and (b) $\text{Fe}_{56}\text{Co}_{40}\text{C}_4$ alloy powders

indicating that 20 hours of milling are enough for a complete diffusion of Cobalt and Carbon atoms into the BCC-Fe lattice. This is consistent with the investigations carried out by Alleg et al. and Zeleňáková et al. [2, 8].

As illustrated in Fig. 2, the lattice parameter of solution shows a decreasing trend within the cobalt content, due to the substitution of Fe (metallic radii, 1.26 Å) by Co atoms (metallic radii, 1.25 Å), into the bcc-Fe structure. These results are in agreement with earlier essays performed on the FeCo alloys [4, 10]. The average grain size does not show a trend lying in the range between 10 nm and 49 nm.

3.3 Scanning electron microscopy

SEM micrographs of the milled powders at 10 and 40 at % Co content are depicted in Fig. 3 a) and b) respectively. During the milling process Fe, Co, and C powders form alloys by

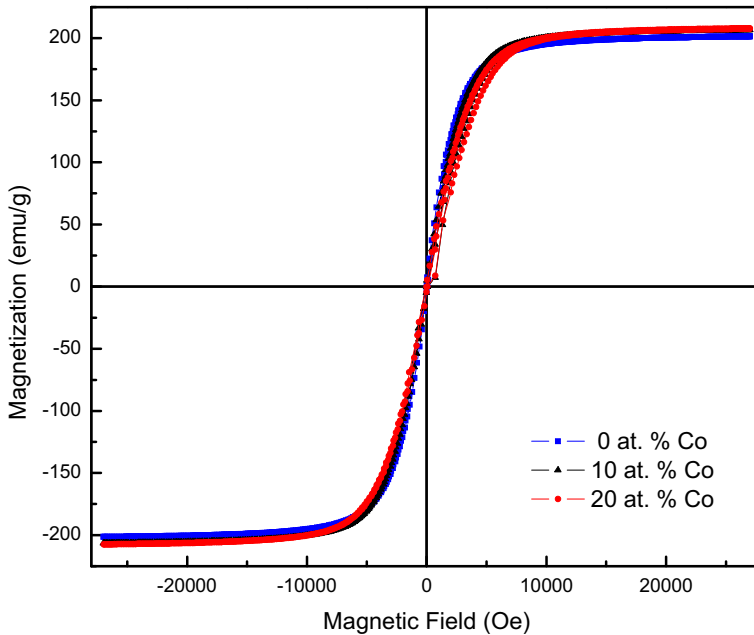


Fig. 4 Magnetization curves for $Fe_{96-x}Co_xC_4$ with $x=0, 10$ and 20

Table 2 Saturation magnetization and coercive field for FeCoC system as function of cobalt content

$Fe_{96-x}Co_xC_4$ (at. %)	M_s (emu/g) (± 2)	H_c (Oe) (± 0.3)
0	211	45.0
10	214	33.4
20	217	49.2
30	217	65.9
40	211	81.8

being continuously submitted to fracture and cold-welding. As a result, both particle size and shape display a non-homogeneous distribution, being the last one independent of cobalt concentration. Also, particle size varies from approximately $0.40 \mu m$ to $50 \mu m$.

3.4 Vibrating sample magnetometer

Figure 4 shows typical hysteresis loops obtained at 300 K for $Fe_{96}C_4$, $Fe_{86}Co_{10}C_4$ and $Fe_{76}Co_{20}C_4$ samples. The saturation magnetization was obtained from them through least squares fitting of the magnetization curves using the classical law approach to saturation [11]. The values obtained are presented in Table 2.

The dependence of the saturation magnetization (M_s) and the coercive field on the Co content is shown in Fig. 5. It can be seen that M_s increases when cobalt content increases until 30 at. % Co and decreases for 40 at. % Co. These results are comparable with earlier studies on the FeCo alloys [8, 10, 12, 13], where the magnetization for this system follows the Slater-Pauling curve (illustrated in Fig. 5), showing a maximum at around 30 at. %

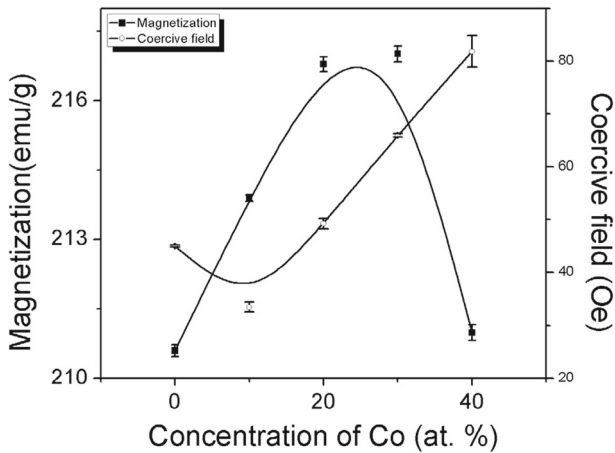


Fig. 5 Saturation magnetization and coercive field of FeCoC vs cobalt content

Co. G. Parette and I. Mirebeau [12] explain this behavior as a crossover of two effects: first, when Co content increase, the Fermi energy is altered because of the number of spins aligned at a specific state density; and second, by the addition of extra electrons in the valence band of the Fe, due to the inclusion of the cobalt atoms (M_s increase), they spin-down, leading to a further decrease of M_s .

On the other hand, the M_s maximum value (217 emu/g) found is slightly smaller than reported by other authors for the compositions evaluated by them [8, 10, 13] whose M_s findings values were in the range of 212 emu/g – 230 emu/g for FeCo alloys obtained by mechanical alloying. The coercive field of the Fe-Co-C system increases as a function of Cobalt content (Fig. 5), this results agree with earlier studies on the FeCo alloys [8, 10]. Despite this, the system still exhibits soft magnetic properties (Table 2).

3.5 Mossbauer spectrometry

Mössbauer spectra and their corresponding hyperfine magnetic field distributions for $\text{Fe}_{96-x}\text{Co}_x\text{C}_4$ alloys system as a function of cobalt content are shown in Fig. 6. The spectra were recorded at room temperature and exhibit a six lines ferromagnetic behavior with broadened lines. The hyperfine parameters are listed in Table 3. The isomer shift data are relative to α -Fe.

The Mössbauer spectrum for 0 at. % Cobalt was fitted using a sextet with a hyperfine magnetic field of 33.0 T and an isomer shift (IS) of 0.008 mm/s, corresponding to a BCC-Fe structure. The spectrum with 10 at. % Co was fitted with three sextets, showing the coexistence of different magnetic environments of Fe, one sub-spectrum with a hyperfine field of 33.8 T corresponding to BCC-FeCoC Fe-rich sites, and the others with 35.0 T and 36.2 T hyperfine fields attributed to Fe substitution by Co. This is consistent with previous results on $\text{Fe}_{50}\text{Co}_{50}$ milled alloys [4, 14].

For higher Co content, the spectra were fitted using a hyperfine field distribution (HFD) showing that the alloys are disordered due to the atomic diffusion of Co and C atoms inside the BCC-Fe structure by mechanical alloying. Figure 6 depicts the hyperfine field distribution for 20, 30 and 40 at. % Co. The distribution consist of one well defined, narrow peak,

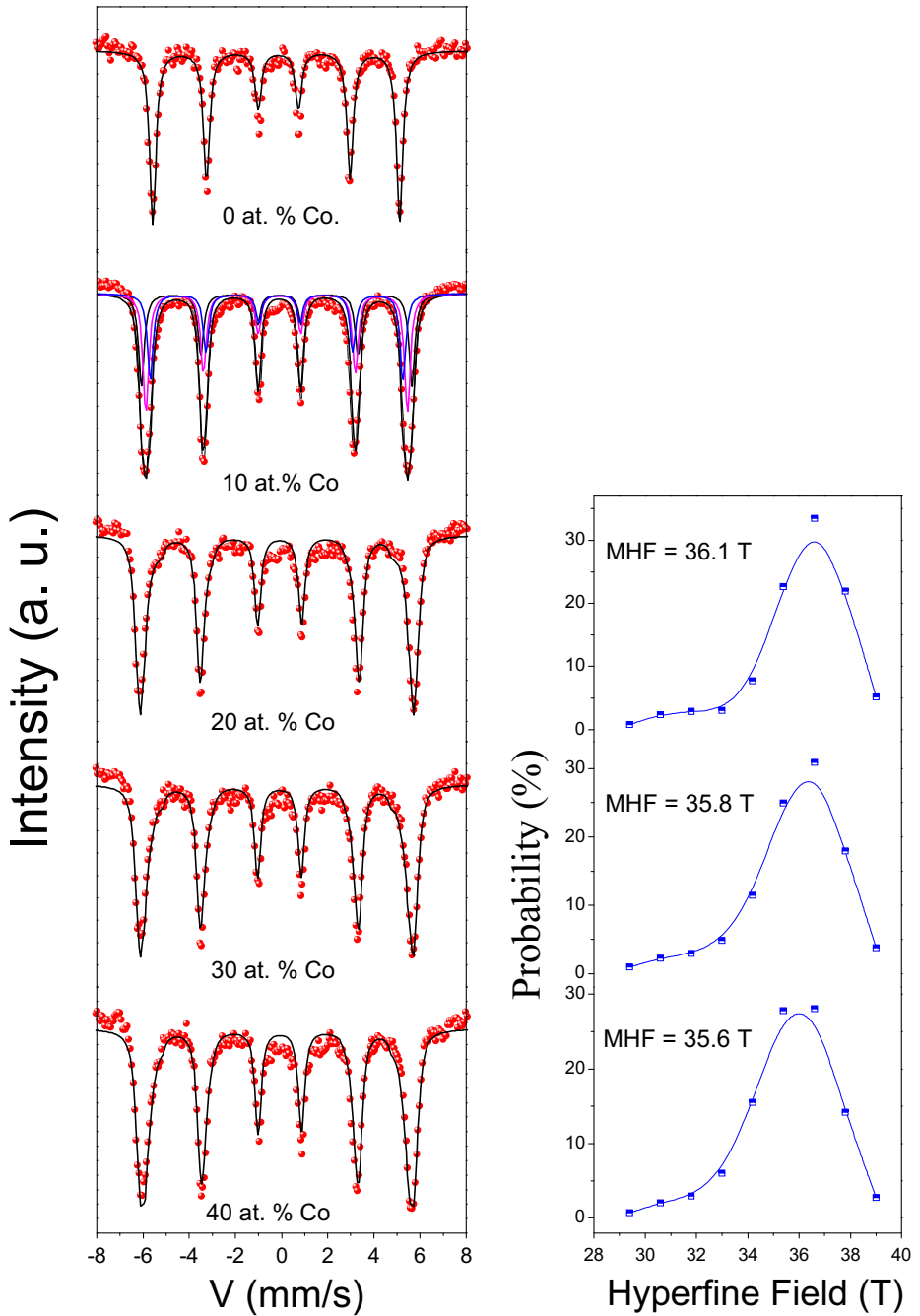


Fig. 6 Mössbauer spectra (*left*) and their corresponding hyperfine fields distribution (*right*) of $\text{Fe}_{96-x}\text{Co}_x\text{C}_4$ with ($x=0, 10, 20, 30$ and 40)

Table 3 Hyperfine interactions parameters of the FeCoC system as a function of cobalt content

Fe _{96-x} Co _x C ₄ (at. %)	Fitting components	IS (mm/s) (±0.02)	QS (mm/s) (±0.02)	HF (T) (±0.5)	% Area	MHF (T) (±0.5)
0	Sextet	-0.01	-0.09	33.0	100	—
10	Sextet 1	0.03	-0.12	36.2	31	35.0
	Sextet 2	0.03	-0.12	35.0	40	
	Sextet 3	0.03	-0.12	33.8	29	
20	HFD	0.04	-0.12	—	100	36.1
30	HFD	0.03	-0.12	—	100	35.8
40	HFD	0.04	-0.12	—	100	35.6

which means that after of 20 h of milling, a relatively homogeneous solid solution was obtained [15]. Additionally, the broadening of the Mössbauer lines and their shift towards higher hyperfine fields are attributed to the presence of Co atoms as first and second nearest neighbors of Fe atoms in the BCC-FeCoC disordered structure. The mean value of hyperfine field for the sample with 30 at % Co is slightly smaller (35.8T) than that reported by Zeleňáková (36.16 T) for 30 wt. % Co [8]. Nonetheless, both Zeleňáková et al and the present work show that when the Co content increases, the mean hyperfine field tends to be nearly constant, approaching to the value reported by Moumeni et al. [14] for Fe₅₀Co₅₀ alloys.

4 Conclusions

The Fe_{96-x}Co_xC₄ system with (X=0, 10, 20, 30 and 40) were synthesized via mechanical alloying. The BCC-FeCoC disordered structure was characterized by X-ray diffraction and Mössbauer spectrometry. The samples showed a soft ferromagnetic behavior for all Co content evaluated. The saturation magnetization and coercivity presented strong dependence on cobalt content. However, carbon content was insignificant in the behavior of these parameters. Some excellent magnetic properties of the system (high magnetization saturation and low coercive field) were obtained; this allows us to use it later as targets in thin films fabrication.

Acknowledgments This work was supported by the Universidad Tecnológica de Pereira. We are very grateful to Ph.D Andres Rosales from Universidad Nacional de Colombia for performing VSM measurements, Ph.D Juan Munoz Saldana from CINVESTAV – Querétaro for EDAX and XRD measurements and Ph.D Humberto Bustos from Universidad del Tolima, for performing Mössbauer spectrometry measurements.

References

- Gonzalez, G., Sagarzazu, A., Villalba, R., Ochoa, J., D'onofrio, L.: Effect of the milling media on the phases obtained in mechanically alloyed equiatomic Fe-Co. *J. Mater Sci.* **360**, 355–360 (2001)
- Alleg, S., Bentayeb, F., Bensalem, R., Djebbari, C., Bessais, L., Greneche, J.: Effect of the milling conditions on the formation of nanostructured Fe-Co powders. *Phys. Stat Sol. (a)* **205**, 1641–1646 (2008)
- Suryanarayana, C., Ivanov, E., Boldyrev, V.: The science and technology of mechanical alloying. *Mater. Sci. A* **304-306**, 151–158 (2001)
- Moumeni, H., Alleg, S., Djebbari, C., Bentayeb, F.Z., Greneche, J.M.: Synthesis and characterisation of nanostructured FeCo alloys. *J. Mater. Sci.* **39**, 5441–5443 (2004)

5. Jartych, E.: On the magnetic properties of mechanosynthesized Co–Fe–Ni ternary alloys. *J. Magn. Magn. Mater.* **323**, 209–216 (2011)
6. Conde, C.F., Borrego, J.M., Blázquez, J.S., Conde, A., Švec, P., Janičkovič, D.: Magnetic and structural characterization of Mo–Hitperm alloys with different Fe/Co ratio. *J. Alloys Compd.* **509**, 1994–2000 (2011)
7. Kawahara, K.: Effect of cold rolling on the mechanical properties of an FeCo–2V alloy. *J. Mater. Sci.* **18**, 3437–3436 (1983)
8. Zeleňáková, A., Olekšáková, D., Degmová, J., Kováč, J., Kollár, P., Kusý, M., Sovák, P.: Structural and magnetic properties of mechanically alloyed FeCo powders. *J. Magn. Magn. Mater.* **316**, e519–e522 (2007)
9. Larson, A.C., Von Dreele, R.B.: General Structure Analysis System (GSAS) Los Alamos National Laboratory Report LAUR 86-748 (2004)
10. Sánchez-De Jesús, F., Bolarín-miró, A.M., Cortés Escobedo, C.A., Torres-villaseñor, G., Vera-Serna, P.: Structural analysis and magnetic properties of FeCo alloys obtained by mechanical alloying. *Journal of Metallurgy*, vol. 2016 Article ID 8347063 (2016)
11. Zhang, H., Zeng, D., Liu, Z.: The law of approach to saturation in ferromagnets originating from the magnetocrystalline anisotropy. *J. Magn. Magn. Mater.* **322**, 2375–2380 (2010)
12. Parette, G., Mirebeau, I.: Magnetic moment distribution in iron-cobalt alloys. *Phys. B* **156–157**, 721–723 (1989)
13. Kim, Y.D., Chung, J.Y., Kim, J., Jeon, H.: Formation of nanocrystalline Fe–Co powders produced by mechanical alloying. *Mater. Sci. Eng. A* **291**, 17–21 (2000)
14. Moumeni, H., Alleg, V., Greneche, J.M.: Structural properties of Fe₅₀Co₅₀ nanostructured powder prepared by mechanical alloying. *J. Alloys Compd.* **386**, 12–19 (2005)
15. Sorescu, M., Grabias, A.: Structural and magnetic properties of Fe₅₀Co₅₀ system. *Intermetallics* **10**, 317–321 (2002)